Physica D 61 (1992) 240–245
North-Holland

PHYSICA D

Singular solutions to the 3D axisymmetric incompressible Euler equations

Alain Pumir[a,b] and Eric D. Siggia[a]

[a]*LASSP, Cornell University, Ithaca, NY 14853-2501, USA*
[b]*LPS, Ecole Normale Supérieure, F-75231 Paris, France*

The problem of development of singular solutions of the 3D Euler equations is considered in the particular case of flows with an axis of symmetry. There is a strong analogy between the physics of such flows, and Boussinesq convection in two dimensions, the buoyancy being replaced by the centripetal acceleration. A hot bubble, initially at rest in cold fluid, tends to rise. During the evolution, strong gradients of temperature develop near the cap of the bubble, while on the sides, vortex sheets tend to roll up. When the cap of the bubble starts folding, a rapid growth of the gradients is observed, suggesting a singularity of the vorticity in the 3D axisymmetric flows like $|\omega|_{\max} \sim 1/(t^* - t)^2$. Analytic estimates for the rate of stretching, consistent with our numerical observations, are provided.

Generation of small scales of motion by a turbulent flow is an important feature of incompressible hydrodynamics at high Reynolds numbers. Understanding this important phenomenon has proven surprisingly difficult, and even very simple questions are still unanswered. As an example, it has been realized for years that vortex lines can be stretched by the flow. Because the stretching results from a nonlinear term, it could conceivably lead to finite time singularities, at least in the inviscid case. Yet, careful numerical studies have suggested that the vorticity grows exponentially, rather than algebraically (i.e., catastrophically). This is the case for the Taylor–Green flow [1], and for antiparallel vortex tubes [2,3], as well as for random initial conditions [4]. These results show that the nonlinear term plays a rather subtle role. Of course, they clearly do not settle the problem of existence of finite time singularities for the 3D fluid equations.

In this paper we present some of our recent results, strongly suggesting the existence of axisymmetric solutions, blowing up in a finite time. This possibility has been suggested by Grauer and Sideris [5]. Our arguments in favor of a singularity are mainly numerical. It is also possible to obtain (nonrigorous) bounds for the rate of growth of the vorticity, useful to understand our numerical results. Technically, in the axisymmetric problem, one has to deal with an essentially two dimensional problem, which leads to obvious simplifications, and allow us to push our calculation much further than in the case of general 3D flows. Physically, a strong analogy exists between the 3D axisymmetric Euler equations and the 2D Boussinesq equations, as we will elaborate below. Although the two systems of equations have very similar structures, it has proven easier technically to study numerically the 2D Boussinesq equations. Our evidence for a finite time singularity comes from our results on the Boussinesq problem. We expect them to hold also for a localized solution of the axisymmetric problem well away from the symmetry axis.

An axisymmetric flow is defined by a velocity field independent of the azimuthal angle, ϕ around the symmetry axis, Oz. The velocity

field, $\boldsymbol{u}(r, z, t)$ satisfies the 3D Euler equations:

$$\partial_t(ru_\phi) + (\boldsymbol{u}_\parallel \cdot \boldsymbol{\nabla}_\parallel)(ru_\phi) = 0\,, \tag{1}$$

$$\partial_t(\omega_\phi/r) + (\boldsymbol{u}_\parallel \cdot \boldsymbol{\nabla}_\parallel)(\omega_\phi/r) = -\frac{1}{r^4}\,\partial_z(ru_\phi)^2\,, \tag{2}$$

$$\frac{1}{r}\,\partial_r(ru_r) + \partial_z u_r = 0\,, \tag{3}$$

$$\omega_\phi = \partial_z u_r - \partial_r u_z\,, \tag{4}$$

where $\boldsymbol{u}_\parallel = (u_r, u_z)$ and $\boldsymbol{\nabla}_\parallel = (\partial_r, \partial_z)$.

Eq. (1) expresses the conservation of circulation around a loop ($r = \text{const}$, $z = \text{const.}$), and eq. (3) is the usual incompressibility condition. The mechanism of generation of azimuthal vorticity, as described in eq. (2), is a consequence of the centripetal acceleration. It is very instructive to compare the system (1)–(4) with the 2D Boussinesq equations with a constant gravity, $\boldsymbol{g} = -g\hat{\boldsymbol{e}}_y$:

$$\partial_t\theta + (\boldsymbol{u}\cdot\boldsymbol{\nabla})\theta = 0\,, \tag{5}$$

$$\partial_t\omega + (\boldsymbol{u}\cdot\boldsymbol{\nabla})\omega = g\,\partial_x\theta\,, \tag{6}$$

$$\partial_x u_x + \partial_y u_y = 0\,, \tag{7}$$

$$\omega = \partial_x u_y - \partial_y u_x\,. \tag{8}$$

A comparison of the two systems of equations shows that the quantity $(ru_\phi)^2$, which is advected by the flow (eq. (1)), plays the same role as the temperature as the source of vorticity (see eqs. (2) and (5)). The "gravity" in the axisymmetric problem is directed radially outwards, and varies with the distance to the axis, r, as $\boldsymbol{g} = \hat{\boldsymbol{e}}_r/r^4$. The velocity field (u_x, u_y) corresponds to (u_z, u_r). Rigorously, this analogy is valid only when the typical length scale of the solution is very much smaller than the distance to the axis, $\bar{r}$. In this case, one has the correspondence

$$(\bar{r}\omega_r,\ \omega_\phi,\ \bar{r}\omega_z) \leftrightarrow (-\partial_x\theta^{1/2},\ \omega,\ \partial_y\theta^{1/2})\,. \tag{9}$$

The analogy between 2D Boussinesq and the 3D axisymmetric problem is of no use to understand the development of singular solutions right at $r = 0$, a possibility we do not consider here.

We have simulated numerically both systems of equations. Since we are primarily interested in simulating solutions developing singularities, our overriding concern is to properly resolve very high gradients. We have used the adaptive mesh techniques that were developed for our previous 3D Euler simulations (ref. [2]). The square $(0, 1)^2$ is mapped onto $\mathbb{R}^2$ by an analytic change of variables. The fields are assumed to vanish at infinity. The "singular structures" we observed are sharp fronts. At least 20–25 mesh points are used to describe a jump. Finite difference techniques are used. With centered finite differences, we occasionally observed unphysical oscillations behind sharp fronts. To suppress the problem, we sometimes used the total variation diminishing (TVD) algorithm [6]. The two algorithms (centered differences and TVD) were compared on a few test problems. Provided the resolution is sufficient, the results obtained with the two algorithms are found to be in very close agreement, thus giving us full confidence in our numerical methods.

To time step, say the Boussinesq equations, the streamfunction ψ, defined by $u_x = \partial_y\psi$ and $u_y = -\partial_x\psi$, was computed at each time step by solving the 2D Poisson equations: $\nabla^2\psi = \omega$. Efficient cyclic reductions methods [7] have been used. The time integration was done by a standard Runge–Kutta–Fehlberg algorithm.

Two extra simplifications are available for studying the 2D Boussinesq equation. First, one can continuously rescale space, time and vorticity in the following way: $X = x/a$, $\Omega = \omega a^{1/2}$, $\Psi = \psi/a^{3/2}$, $\theta = \Theta$ and $\partial_T t = a^{1/2}$. The equations then read

$$\partial_T\Theta + \alpha\boldsymbol{X}\cdot\boldsymbol{\nabla}_X\Theta + \frac{\partial(\Psi, \Theta)}{\partial(X, Y)} = 0\,, \tag{10}$$

$$\partial_T\Omega + \alpha\boldsymbol{X}\cdot\boldsymbol{\nabla}_X\Omega + \tfrac{1}{2}\alpha\Omega + \frac{\partial(\Psi, \Omega)}{\partial(X, Y)} = \partial_X\Theta\,, \tag{11}$$

with the definitions

$$\nabla_X^2 \Psi = \Omega\,, \quad \alpha = -\frac{1}{a}\,\partial_T a\,. \tag{12}$$

As is the case for the nonlinear Schrödinger equation, continuously rescaling the solution is a very efficient way to maintain appropriate resolution while simulating a solution collapsing down to very small scales [8].

Also, in the Boussinesq case, it is possible to maintain the maximum gradient in the region where the resolution is highest by simply subtracting the velocity of the point where the gradient is largest.

In the 3D axisymmetric case, the Galilean invariance and the possibility to continuously rescale the solution are lost. These properties make the numerical study of the Boussinesq equations much easier. In the following, we will restrict ourselves to the Boussinesq equations. A more complete description of our results can be found elsewhere [9].

Although we have simulated a whole range of initial conditions, we will discuss here only the problem of a single bubble, initially at rest ($\omega = 0$ everywhere). More specifically, our initial condition was $\theta(x, y) = (1 + 0.2y)/(1 + x^2 + y^2)^2$. This configuration is symmetric with respect to $x = 0$.

Qualitatively, hot regions tend to rise into colder regions. This situation is somewhat reminiscent of the 1D Burgers equation, where a similar mechanism leads to shocks in a finite time. Here of course, the incompressibility makes the problem much more subtle[#1]. The initial stages of the evolution lead to a region of sharp gradients ahead of the bubble, because of the tendency of hot regions to rise in colder regions. After a while, a front separating a zone of high temperature underneath a zone of low temperature develops. In the process, fluid of intermediate temperature is expelled, leading to a jet on each side of the cap. This leads to the formation of arms of warm fluid, that eventually tend to roll-up.

Quantitatively, we found that the temperature gradient at the tip of the bubble was growing first slower than exponentially. In this (slow) regime, the maximum gradient grew by a factor 100 (see fig. 1).

A qualitative change occurs around $t = 8.5$. In fig. 1, the temperature gradient starts growing much faster than exponentially. Our data shows that the gradient grows like $1/(t^* - t)^2$, over 4 orders of magnitude (see fig. 1b). When we stopped our calculations, there was no obvious impediment to further integration. In physical space, this change of regime is characterized by the development of an instability on the cap of the bubble. Fig. 2 shows the right part of the interface shortly after the instability starts. The following collapse happens at the tip of the bubble, and proceeds by a series of repeated foldings while the width of the interface is rapidly decreasing. Figs. 3 and 4 show details of the shape of the bubble, closer to the singular time ($\max|\nabla\theta| = 1.55 \times 10^3$), and at a much smaller scale. The foldings keep reducing the radius of curvature, r_c, so as to have always $r_c \sim \sigma$, where σ is the width of the interface, as it is in figs. 3, 4, near the region where the gradients are the largest. There is an obvious similarity with the physical picture that was found in the study of vortex filaments, described by the Biot–Savart model [11].

After each folding of the interface, a new inflection point develops on the front. The appearance of an inflection point always seemed to trigger a roll-up of the vortex sheet. This mechanism leads to the development of spirals at all

[#1] The effect of the incompressibility constraint on the nonlinear mechanism leading to shock formation in the Burgers equations can be studied in the 2D convection in porous media. The equations of motion are

$$\boldsymbol{u} = \theta \hat{\boldsymbol{e}}_y + \nabla p\,,$$

$$\nabla \cdot \boldsymbol{u} = 0\,,$$

$$\partial_t \theta + (\boldsymbol{u} \cdot \nabla)\theta = 0\,.$$

These equations lead to the formation of steep interfaces, and to finite time singularities. The gradients of θ grow like $1/(t^* - t)$ [10].

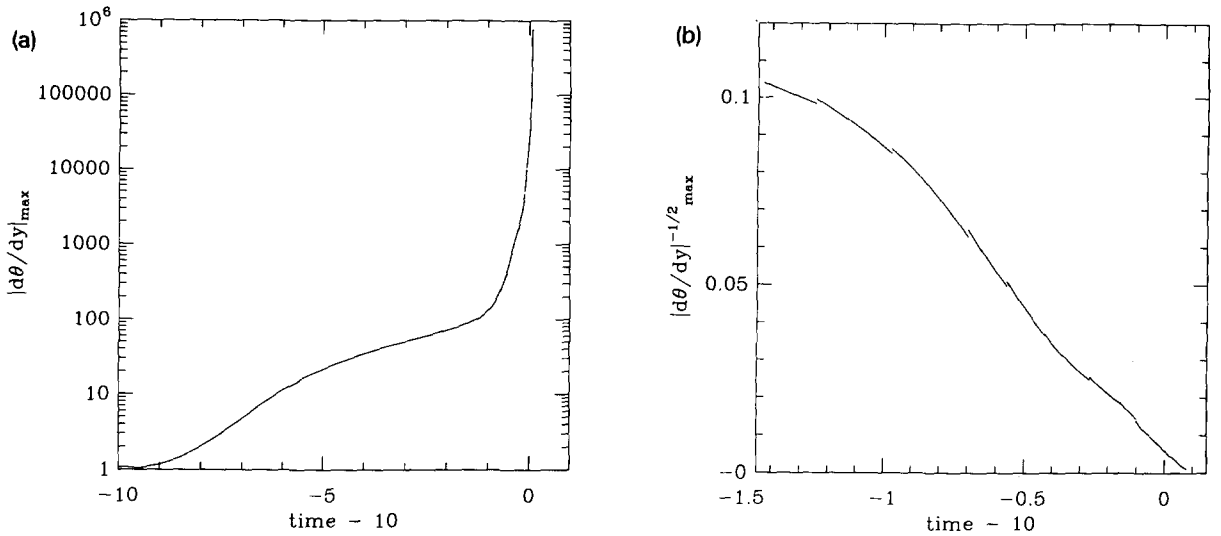

Fig. 1. The maximum of $|\partial_y\theta|$ evaluated on the axis of symmetry ($x = 0$) (a) and its inverse square root (b) as a function of time. Note that time has been shifted by 10. Only the asymptotic regime where $|\partial_y\theta| \sim 1/(t^* - t)^2$ is shown in (b).

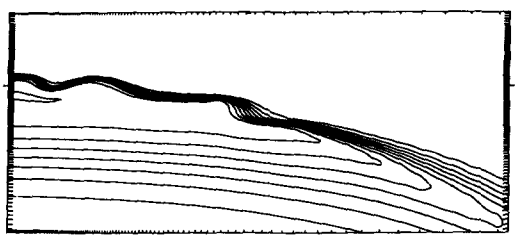

Fig. 2. The shape of the cap of the bubble at time $t = 8.75$, shortly after the first destabilization of the bubble cap ($|\nabla\theta|_{max} = 137$). Iso-$\theta$ lines are shown here. The contour lines run from 0.1 (ahead of the front) to 1. Only the right half of the bubble is shown here. The x-coordinate range is $0 \le x \le 0.1$ and the y-range is a third of the x-range.

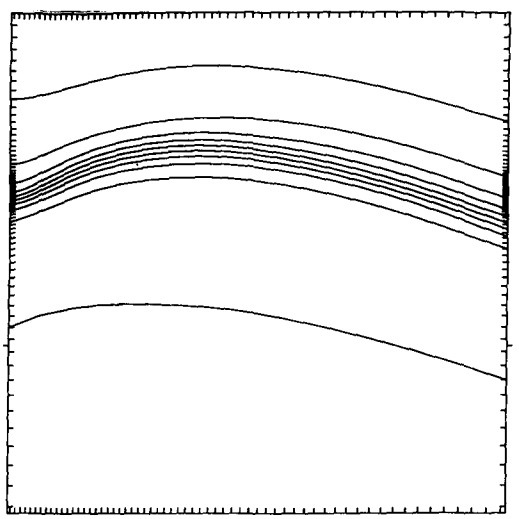

Fig. 3. The shape of the cap of the bubble at time $t = 9.74$ ($|\nabla\theta|_{max} = 1.55 \times 10^3$). Iso-$\theta$ lines are shown. The contour lines run from 0.1 to 0.9. The right half of the bubble is shown here, and the x-coordinate range is $0 \le x \le 0.029$, and the y-range is a third of the x-range.

scales, separating almost horizontal regions where a local maximum of the gradient grows. It was found that the stretching acting on one local maximum was predominantly due to neighbouring regions of the flow. In the late stages of the evolution, the vorticity grows approximately like $|\omega| \sim 1/(t^* - t)$. The temperature jump between the front and the back of the front decreased steadily during the evolution. When we stopped our simulation the maximum gradient had grown by a factor 10^6, whereas the total jump in θ across the interface had decreased by a factor 3 only. It is possible to fit our solutions with the following functional dependencies:

$$\theta = \theta_0 + (t^* - t)^{\eta} f(x/(t^* - t)^{2+\eta}, \tau), \qquad (13)$$

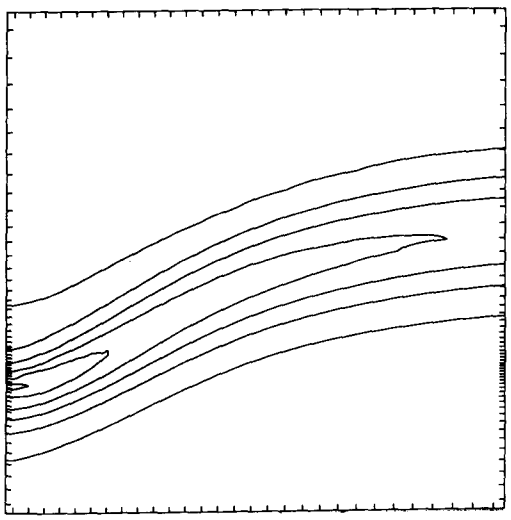

Fig. 4. The quantity $|\nabla\theta|$ at the same time as in fig. 3. The scales have been blown up by a factor of 3, compared to fig. 3. The contour interval is 240. The tick marks along the perimeter show our numerical mesh points. A similar resolution has been maintained around the region where we decided to follow the maximum gradient.

$$\omega = 1/(t^* - t) g(x/(t^* - t)^{2+\eta}, \tau) , \tag{14}$$

where $\tau = -\ln(t^* - t)$ and a small value of η: $\eta = 0.2 \pm 0.2$. Note that the Boussinesq equations are consistent with the scalings of eqs. (13), (14). It is much harder to actually find solutions for f and g. Our calculations suggest that they remain time dependent, arbitrarily close to the singular time.

Useful analytic estimates can be obtained by ignoring the actual shape of the interface, and using a contour dynamics limit. In this approximation, one describes the front by a temperature discontinuity, located on a curve $x(\lambda, t)$, where λ is a Lagrangian parameter. Because of the buoyancy term, circulation is generated on the curve $x(\lambda, t)$. The velocity $u(\lambda, t)$ and the circulation $\gamma(\lambda, t)$ are related in the contour dynamics limit by the following equations:

$$u_i(x, t) = g\epsilon_{ij}\, \partial_j \int \ln|(x - x(\lambda, t)|\gamma(\lambda)\, \frac{d\lambda}{2\pi} , \tag{15}$$

$$\gamma(\lambda, t) = \int_0^t \partial_\lambda y(\lambda, t')\, dt . \tag{16}$$

Here, ϵ_{ij} is the completely antisymmetric tensor ($\epsilon_{12} = 1$, etc.), and $x_1 \equiv x$, $x_2 \equiv y$. The stretching, responsible for the growth of the gradients is given by

$$D_t|\nabla\theta|^2 = -2\nabla\theta \cdot e \cdot \nabla\theta , \tag{17}$$

where D_t denotes the Lagrangian derivative and $e_{ij} = (\partial_i u_j + \partial_j u_i)/2$ is the rate of strain tensor. From eqs. (15)–(17), the following equation for the stretching can be derived:

$$\partial_t|\nabla\theta|^2 \sim c \int_0^t |\nabla\theta|^2 \kappa(t')\, dt' , \tag{18}$$

where κ denotes the curvature of the interface (see ref. [9] for details). Eq. (18) is useful to understand qualitatively the dynamics in the two regimes we found numerically. Before the cap of the bubble starts breaking up, $\kappa \sim$ const., and eq. (18) predicts that $\nabla\theta$ grows exponentially. When the instability starts, our numerical results suggest that $\kappa(t) \sim |\nabla\theta|$. This has to be understood in a statistical sense, since we never reached a truly self-similar state. In this case, it is easy to show that eq. (18) leads to a growth asymptotically like: $|\nabla\theta| \sim 1/(t^* - t)^2$.

One of the most crucial mechanisms leading to the eventual singularity is the destabilisation of the cap of the bubble (see eq. (18)). It is well known that a front at rest separating hot fluid, underneath cold fluid is intrinsically unstable (Rayleigh–Taylor instability). In the case of a curved, rising front, the stretching induced by the motion of the fluid tends to strongly restabilize the instability, as it has been discovered in the case of curved flame fronts [12]. The main physical consequence is that the interface separating hot and cold fluids remains stable for surprisingly long times. However, as the interface becomes thinner and thinner, it must eventually become unstable. A similar prediction was made by Batchelor, in an analogous context [13].

Because our problem is intrinsically time-dependent, there is a source of noise at the level of the cap of the bubble. A simple analytic treatment of the stability problem (see ref. [9]) gave a good estimate of the time when the instability developed. We are therefore confident that the instability is real, and is not a numerical artefact.

In the case of 3D axisymmetric Euler flows, the analogy with 2D Boussinesq convection suggests a divergence of the magnitude of the 3D vorticity, $\|\omega\|_\infty$, like $|\omega| \sim 1/(t^* - t)^2$ (see eq. (9)). The velocity itself remains finite. Because of the bounds found by Leray [14], which show that the velocity has to diverge if a solution of the Navier–Stokes equations is to diverge, we expect that our singular solutions will not survive in the viscous case. It is also expected that the axisymmetric solutions we found are completely unstable with respect to non axisymmetric perturbations. Some of the quantitative aspects of our solutions may very well apply to more general initial conditions. The salient features of our simulations are the formation of vortex sheets and their repeated destabilisation, leading to the roll-up of the interface. Indeed, formation of vortex sheets has been observed in all the simulations of the 3D Euler equations we are aware of. The roll-up of vortex sheets will lead to the formation of vortex tubes, a structure that has been reported many times in the study of 3D incompressible turbulence. It would be interesting to understand whether the physical mechanisms involved in the case of 3D axisymmetric flows have anything to do in the general 3D Euler initial value problem.

We are grateful to R. Grauer and T. Sideris for having communicated their results to us. Our computations were done on RISC 6000 workstations donated by IBM. Support from the Air Force Office of Scientific Research under Grant number 91-0011 and the National Science Foundation under grant number DMR-9012974 are gratefully acknowledged.

References

[1] M. Brachet, D. Meiron, B. Nickel, S. Orszag and U. Frisch, J. Fluid Mech. 130 (1983) 411.
[2] A. Pumir and E.D. Siggia, Phys. Fluids A 2 (1990) 220.
[3] D. Meiron and M. Shelley, preprint (1990).
[4] M. Brachet, M. Meneguzzi, H. Politano, P.L. Sulem and A. Vincent, private communication.
[5] R. Grauer and T. Sideris, Phys. Rev. Lett. 67 (1991) 3511.
[6] For a general discussion, see C.B. Laney and D.A. Caughey, A.I.A.A. paper 91-0632, 29th Aerospace Sciences meeting, Reno, NV, Jan. 1991;
We have used the algorithm described by S. Osher and S. Chakravarty, SIAM J. Numer. Anal. 21 (1984) 955.
[7] P.N. Swartzrauber, SIAM Review 19 (1977) 490.
[8] B. LeMesurier, G. Papanicolaou, C. Sulem and P.L. Sulem, Physica D 31 (1988) 78.
[9] A. Pumir and E.D. Siggia, Phys. Fluids A 4 (1992) 1472.
[10] A. Pumir, B. Shraiman and E.D. Siggia, Phys. Rev. A 45 (1992) 5351.
[11] A. Pumir and E.D. Siggia, Phys. Fluids 30 (1987) 1606.
[12] Ya. B. Zeldoich, A.G. Istratov, N.I. Kidin and V.B. Librovitch, Combust. Sci. Techn. 24 (1980) 1.
[13] G.K. Batchelor, J. Fluid Mech. 184 (1987) 399.
[14] J. Leray, Acta Math. 63 (1934) 193.